

Analysis of Thermal Images for the Detection of Diabetic Foot

Nithya Rajagopalan*, Nirmala K*, Sivagami Vishnukumar*, Srija Vaidyanathan* and Sasi Preethi*

*Sri Sivasubramaniya Nadar College of Engineering, Chennai, Tamil Nadu, India, nithyar@ssn.edu.in

ABSTRACT:

Diabetes mellitus is one of the most commonly diagnosed disorders around the globe. Around 400 million people globally are affected with this disorder with around 1.2 million deaths. Some complications include diabetic retinopathy, foot ulcers, and renal failure. The use of thermal imaging makes the diagnostic process non-invasive, reducing discomfort and the risk of infection associated with traditional methods. Early detection of diabetic foot ulcers is crucial for timely intervention and prevention of severe complications, such as infections and amputations. Deep learning models have the potential to provide accurate diagnoses by analyzing thermal patterns that may not be easily discernible by the human eye and could potentially track the progression and severity of the disease over time. A total of 996 images with 264 healthy images and 732 unhealthy RGB images were used in this work. The total dataset was split into training, testing, and validation groups in the ratio 6:2:2. The left and right foot images were equally randomized in the respective models while training. ResNet50 is used with a learning rate of 0.01 having 20 epoch gives the highest accuracy of 98% and a minimum loss of 1% further, the work can be enhanced with a real-time database.

1. Introduction

Diabetes mellitus or Diabetes is caused by the irregular secretion of insulin in the body that alters the levels of glucose present in the blood. The alteration in the level of glucose caused by the variation of insulin is known to have detrimental effects on the heart, blood vessels, nerves, eyes, and kidneys leading to lifelong issues such as cardiovascular diseases, peripheral nerve damage, renal failure, diabetic retinopathy, and diabetic foot ulcers. Diabetic Foot Ulcer (DFU) is a type of skin ulcer that occurs as the diabetes progresses. The skin ulceration covers the lower limb of the patient. Complications of diabetic foot ulcers lead to osteomyelitis and gangrene [1]. In extreme cases of DFU, a patient's leg is amputated to prevent further complications. Factors that contribute to DFU include Diabetic Neuropathy and Peripheral Artery Disease [2]. In Neuropathy, Hyperglycemia induces oxidative stress on the nerve cells which triggers neuropathy. Further glycosylation leads to ischemia. Neuropathy occurs at the sensory, motor, and autonomic levels [2]. Damage to the motor neuron causes muscular neuropathy resulting in the paralysis of flexor extensor muscles such as the Extensor Digitorum Brevis. This muscular immobilization often results in anatomical changes in the foot arch and the metatarsophalangeal joints [3] leading to deformities of the foot such as Plantar Aponeurosis, Claw Toe, and Horseshoe foot [4]. Sensory neuropathy is accompanied by muscular neuropathy causing pain insensitivity, the patient loses their ability to perceive pain increasing the susceptibility to injuries without consciousness, Sensory neuropathy also results in unequal foot load and an imbalance in the patient's gait. At the autonomic level, reduction in sweat secretion and overheating of the skin occurs due to increased perfusion leading to skin breakdown. With increased friction and skin abrasion, pressure ulcers are aggravated and there is a compromise in the body's natural immune response to foreign bodies [5][1].

According to Xuan Wang et al [3], 78% of all patients diagnosed with DFU already have Peripheral Arterial Disease. At the cellular level, excessive blood sugar levels cause the dysfunction of endothelial cells which reduces the levels of vasodilators in the blood. With time, reduced vasodilation levels contribute to vasoconstriction and hypercoagulation which results in ischemia and skin ulceration. Because of the endothelial dysfunction, re-vascularization ability becomes limited and the wound healing process is slow. DFUs are classified based on the wound progression depending on the site, size of the ulceration, and depth of the wound [5]. This deterioration increases the mortality rate significantly and therefore requires amputation. According to et al, amputation due to DFU happens every 30 seconds in the world as an intervention to prevent gangrene from taking over the patient's lower limb entirely.

DFU has been shown to negatively impact the health-related quality of life in patients suffering from diabetes-related complications. In a variety of studies conducted to understand the patient-reported outcomes associated with diabetes, reduced mobility and the resulting loss of independence [6] in carrying out day-to-day life activities were identified as contributing factors for a lower quality of life. Additionally, the worries associated with infection and wounds and the fear of amputation [7] increased anxiety and depression among the patients. These psychosocial determinants showed a high correlation with a reduced health-related quality of life [8] and were shown to severely impact the mood and overall living in patients apart from the physical injury itself. With the aim of wound healing and preventing further deterioration of the ulcers leading to amputation there are several multidisciplinary control measures in the form of diagnosis and treatment that are in practice clinically. Tools for diagnosis are foot examinations, patient history evaluations, and physical examinations [9]. Certain biomarkers with an indication for inflammation such as the Tumor Necrosis Factor - α , Procalcitonin, and Interleukins

[10] are also currently in use. The treatment option for DFUs is removal of debridement, in more severe cases surgical debridement is preferred. Other treatment interventions include wound dressings; antibiotics are also administered based on the type of infection and type of pathogen present [9].

Over half of the world's population is diagnosed with diabetes. In 2021 alone, 536 Million people suffered from diabetes, and the prevalence is set to grow by 12.2 % and is expected to affect 783.2 Million people by the year 2045 [11]. 10 to 15 % of the population suffering from Diabetes are susceptible to developing a DFU [4], the chances of which are 25 % during a diabetic patient's lifetime [1] with an incidence rate of 2 % annually [12]. Routine screening of the patient's foot is necessary for proper management of the ulcer deterioration and monitoring of the wound healing process. The patient has to make visits to their practitioner every 1 year or 3 to 6 months depending on their risk category [12]. This means that a heavy economic burden is placed on the patient as well as the hospital. With the risk of reinfection and amputation, an average 5-year mortality rate for a patient suffering from DFU stands as high as 40% [13] making it one of the most common causes of death globally. Hence, early diagnosis of DFUs is important in order to improve the quality of life of patients and prevent death and more tools have to be innovated for timely identification and intervention [14].

Currently the DFU are diagnosed by inspecting the toes, toenails and foot for any potential ulcer-causing injuries. Blood flow rates in the foot are evaluated by feeling the pulse and the sensitivity of the foot is also diagnosed. Ultrasound Doppler test is performed to analyze the blood vessel and the blood flow [15]. All the state of art methods involve certain procedures and are not suitable for early diagnosis. To overcome the limitations of these methods a non-invasive approach of screening is suggested using thermal imaging [16]. Detection of diabetic foot ulcers using thermal imaging helps to reduce the progression of the disease at the early stage thereby avoiding the foot complications that may lead to severe ulceration and amputation of fingers and toes [17]. The scope of this work is to provide a dedicated non-invasive testing tool for the diagnosis of Diabetic foot ulcer. While using non-invasive techniques such as thermal imaging reduces the discomfort caused to the patient and improves the early diagnosis rate significantly. This thermal imaging diagnostic tool will be an effective tool during mass screening. The accuracy associated with such techniques in its ability to distinguish Diabetic foot ulcers with other kinds of foot pressure sores is still a major challenge where current research works are focusing on [17].

Thermal cameras detect and capture various degrees of infrared light to determine temperature. Thermal imaging is a relatively safe way to make early decisions about a bosom disease that does not involve injecting any energy into the human body [17][18]. Thermographic cameras distinguish long-infrared radiation (approximately 9,000-14,000 nanometers or 9-14 m) producing thermograms, which are visual representation of this radiation [19]. It represents a visual depiction of temperatures in order to compare them. Forward-looking infrared cameras, as well as other warm imaging cameras, use the location of infrared radiation, which is typically transmitted from an intensity source (thermal radiation), to create a picture for video yield. The two primary wavelengths of infrared light are long-wave and medium-wave infrared light. Long-wave infrared (LWIR) cameras, often known as "far-infrared" cameras, operate at a wavelength of 8 to 12 m and may detect heat sources as far as a few kilometers away, such as hot engine parts or human body heat. Objects in the 3-5m range are detected using medium-wave infrared (MWIR) cameras [19][20]. In this work, a method for an early and non-invasive way of detecting diabetic foot through the use of thermal imaging and deep learning techniques is presented. Introduction and early research are discussed in section 1 followed by the methodology in section 2. The simulated results and performance analysis is addressed in section 3.

2. METHODOLOGY:

The methodology to detect diabetic foot ulcers involves data acquisition using a FLIR camera [21] followed by preprocessing of the acquired images. The acquired images are augmented and rescaled then fed to the CNN model to classify the diabetic foot from the control group. The overall methodology is presented in Fig 1.

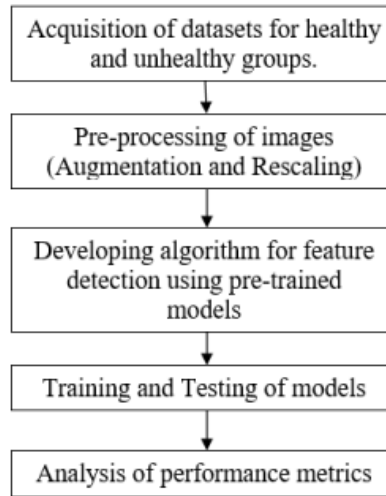


Fig 1: Overall Methodology

2.1 Dataset and Preprocessing

The images are obtained from the Plantar thermogram database [22] with 122 diabetic subjects and 45 control subjects. The total dataset was split into training, testing, and validation groups in the ratio 6:2:2. The left and right foot images were equally randomized in the respective models while training. Since the actual dataset contained segments of the foot (angiosomes) as well, segregation of the whole foot image from the angiosomes was done in order to maintain uniformity, and data augmentation was performed to increase the sample space after segregation. Fig 2. Shows a sample image of both healthy and unhealthy feet.

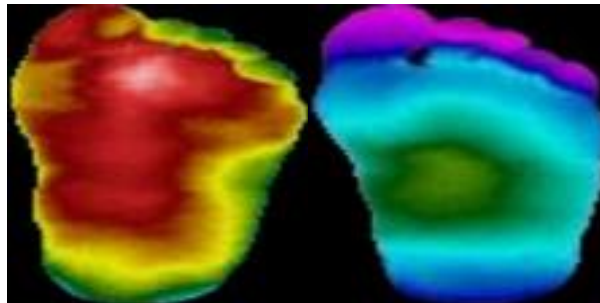


Fig. 2. Healthy (left) and Unhealthy (right) image sample

In order to maintain the uniformity of the dataset and to match the size of the original sample space, resizing and data augmentation is performed on the dataset. The rotation range defines the angle at which the image is rotated along its vertical axis [18][21]. For the considered dataset, a value of 40 is set as the rotation range. The shear range is the amount of shear change given to a particular axis alone while the other axes remain intact. A minimal value of 0.2 as a shear range is used to prevent loss of information. The horizontal flip was set to 0.2. It is responsible for flipping the rows and columns in a horizontal orientation. Zooming and brightness ranges were set to 0.2 and (0.5, 1.5) respectively. After augmentation a total of 996 images with 264 healthy images and 732 unhealthy RGB images were used in this work.

2.2 CNN-based Image Classification

The pre-processed images are fed into multiple pre-trained models such as AlexNet, VGGNet, InceptionNet, MobileNet, and ResNet50. After multiple levels of training and validation, the performance metrics are compared against one another in order to determine the best model for the diagnosis of DFU.

2.2.1 AlexNet:

AlexNet is a renowned deep convolutional neural network architecture, Fig.3 comprising five convolutional layers and three fully linked layers. Within the convolutional layers, filters of different sizes are used to extract features from input images. Furthermore, max-pooling layers are used to reduce the feature maps' spatial dimensions, while the fully connected layers play a pivotal role in the ultimate classification process. AlexNet's success can be attributed to the adoption of convolutional neural networks with deep layers using ReLU activation functions, which facilitated the model to learn more sophisticated features than previous approaches [23].

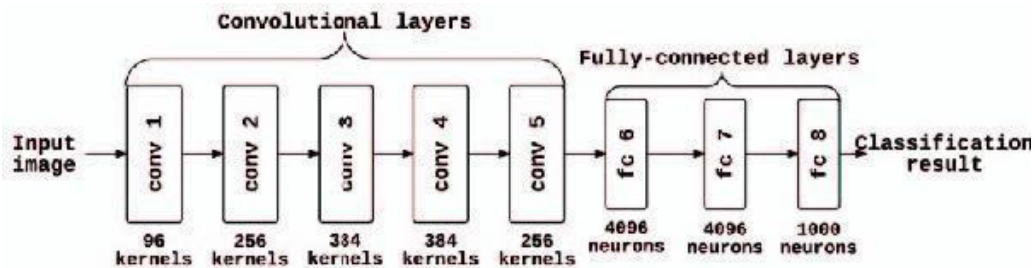


Fig. 3. Architecture of AlexNet [Shafiq S, 2021]

AlexNet was trained using stochastic gradient descent (SGD) with momentum, and weights were updated using back propagation. The model was developed using a specific classification task after being fine-tuned on a huge collection of images, such as Image Net. [23][24].

2.2.2 VGGNet:

VGG16 is a convolutional neural network architecture, Fig.4, comprising 19 layers, including 16 layers of convolution and 3 layers that are fully connected, and is designed to learn high-level features from input images and classify them into various categories. VGG16 is a large network with approximately 138 million parameters. A pooling layer is added after a few convolutional layers which decreases the height and width. There are approximately 64 filters accessible, which are used to double to approximately 128 and finally to 256 filters. 512 filters are used in the final stages [24][25].

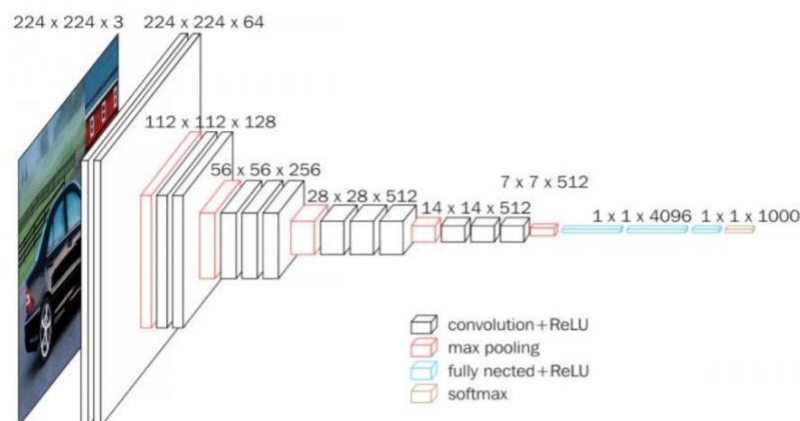


Fig. 4. Architecture of pre-trained VGG19 model [Mohammed Y, 2021]

2.2.3 Inception Net:

The network is built with around 22 layers, Fig 5. The use of average pooling before the classifier allows to easily adapt and fine-tune our networks for other label sets. Rectified linear activation is used in all convolutions, including those within the Inception modules. Deep depth and the ability to effectively propagate gradients back through all layers is complex in this network [23][26][27].

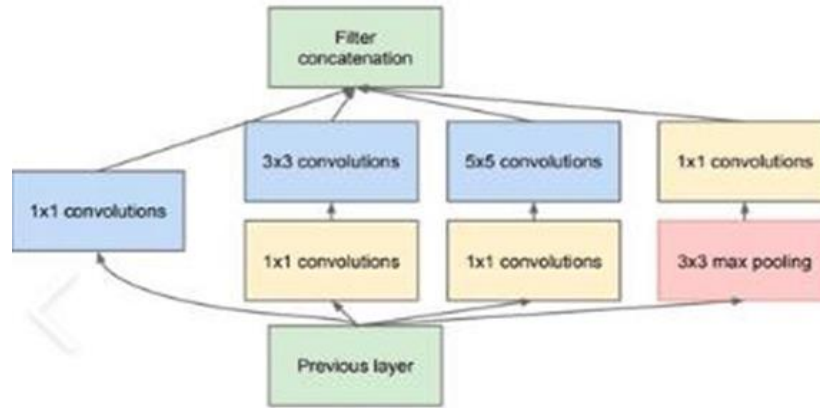


Fig. 5. A flowchart describing the architecture of Inception

2.2.4 Mobile Net:

The MobileNet model, as shown in Fig. 6, is constructed based on a combination of depthwise separable convolutions and pointwise convolutions. Depthwise separable convolutions consist of two layers: depthwise convolutions, which used to apply a single filter to every incoming channels. After that, the pointwise convolution—a straightforward 1x1 convolution—is used to linearly merge the output of the depthwise layer. MobileNets uses batch normalisation and ReLU nonlinearities for both layers. All layers are followed by batch normalisation and ReLU nonlinearity, with the exception of the last fully connected layer, which lacks nonlinearity and connects to a softmax layer for classification. It's worth noting that MobileNet comprises a total of 28 layers when counting depthwise and pointwise convolutions separately.

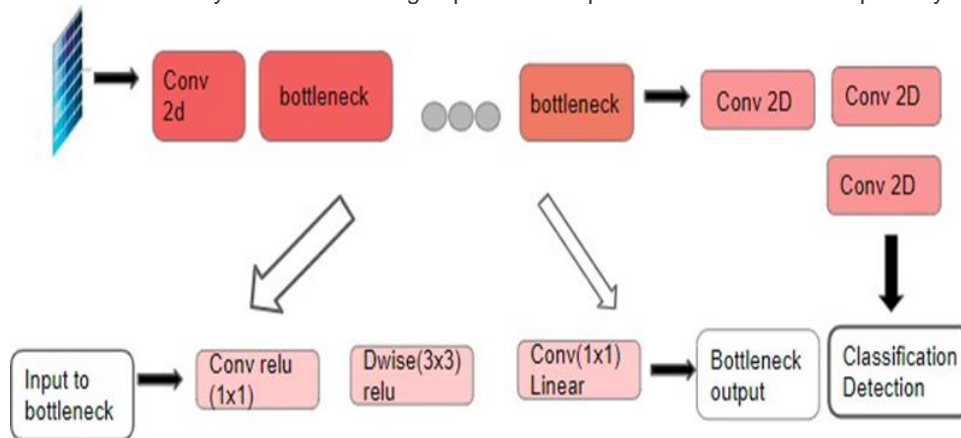


Fig. 6. A flowchart describing the architecture of MobileNet [Howard 2017]

2.2.5 Resnet 50:

ResNet50 is an architecture, Fig. 7, of a deep convolutional neural network that encompasses 50 layers. These layers include layers that are convoluted, max-pooling layers, and fully connected layers, where filters of various sizes are utilized to obtain essential information from the input data. The fully connected layers perform the final classification, and the max pooling layers assist in reducing the spatial dimension of the map's features. ResNet50 is typically trained using

stochastic descent of gradients(SGD), and the weights are updated using backpropagation. Its innovation in the use of residual connections has enabled it to learn deeper representations of images and mitigate the vanishing gradient problem in very deep networks [23][24].

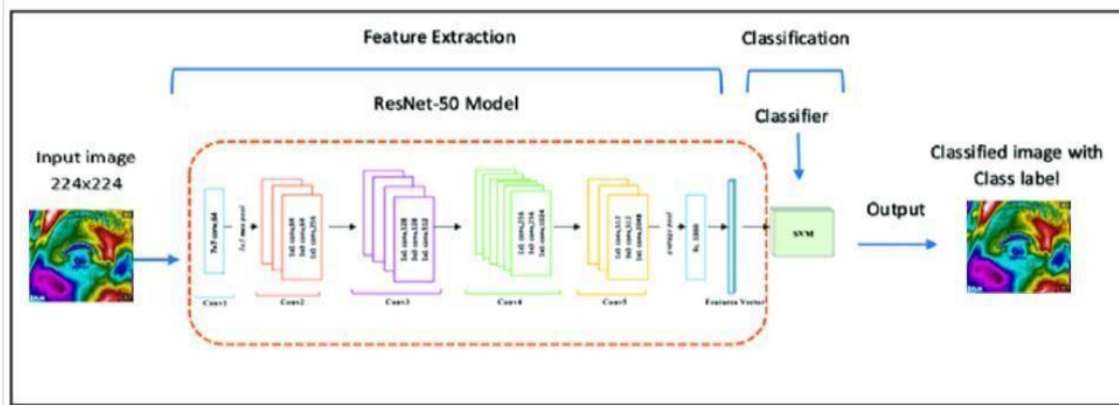


Fig.7. ResNet Architecture [Rammah Yousef, 2022]

3. RESULTS AND DISCUSSION

The dataset considered for this work were preprocessed and fed to the different CNN architecture namely Alexnet, VGG net, mobilenet, Inception and Resent50 and the performance of each architecture are analyzed. The transfer learning is performed on the specified models for classification of DFU and healthy subjects. The hyper parameters of the pre-trained models are tuned manually for better classification thereby increasing the efficiency of the models. The learning rate and the epochs of the model are considered for tuning. The performance metrics for each model are presented in Table 1 and 2.

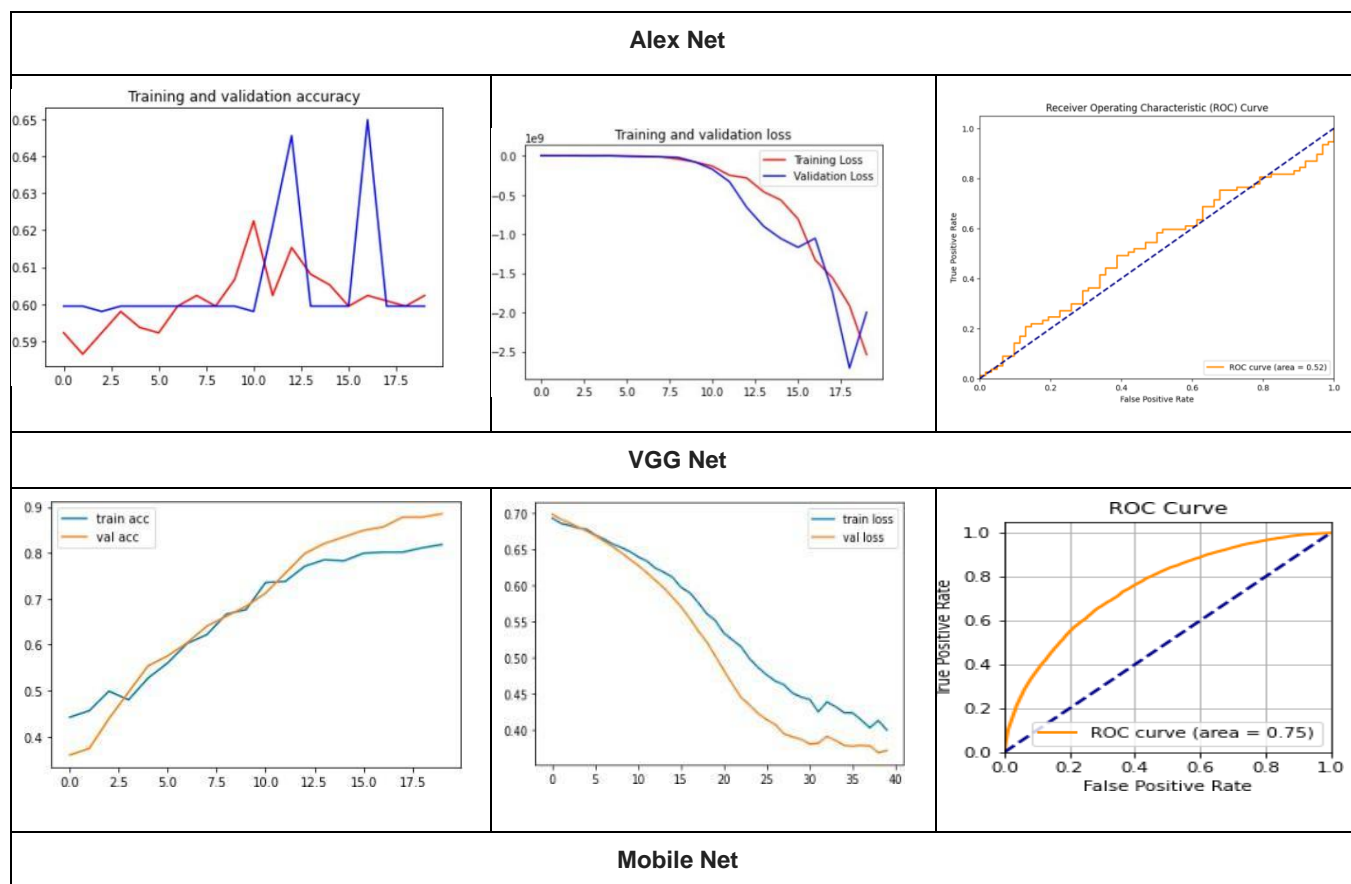
Table 1. Training and validation accuracy for AlexNet and VGGnet

Learning rate	Epochs	Alexnet		VGG16	
		Training Accuracy	Validation Accuracy	Training Accuracy	Validation Accuracy
0.001	35	0.6556	0.6915	0.85	0.84
0.001	30	0.6530	0.6818	0.89	0.85
0.001	25	0.6533	0.6766	0.81	0.91
0.001	20	0.6523	0.6994	0.82	0.92
0.01	20	0.6203	0.6988	0.86	0.79
0.1	20	0.6199	0.6734	0.57	0.55

Table 2. Training and validation accuracy for MoblieNet, Inception and Resnet 50

Learning rate	Epoch	Mobile net		Inception		Resnet 50	
		Training Accuracy	Validation accuracy	Training Accuracy	Validation accuracy	Training Accuracy	Validation accuracy
0.01	5	0.760	0.965	0.78	0.90	0.734	0.9176
0.01	10	0.780	0.94	0.76	0.87	0.71	0.9325
0.01	30	0.960	0.859	0.8	0.89	0.92	0.8311
0.01	20	0.992	0.938	0.86	0.95	0.99	0.9649
0.1	20	0.965	0.947	0.75	0.82	0.9659	0.94
0.001	20	0.939	0.965	0.88	0.82	0.9348	0.9750
0.25	20	0.948	0.859	0.90	0.85	0.9572	0.8346

From the table 1 and 2 it can be inferred that the different hyper parameters such as learning rates, epochs and optimizers are used in training the CNN models (AlexNet, VGGNet, InceptionNet, ResNet50 and MobileNet). From the analysis, it is understood that the ReseNet50 outperforms the other considered models.



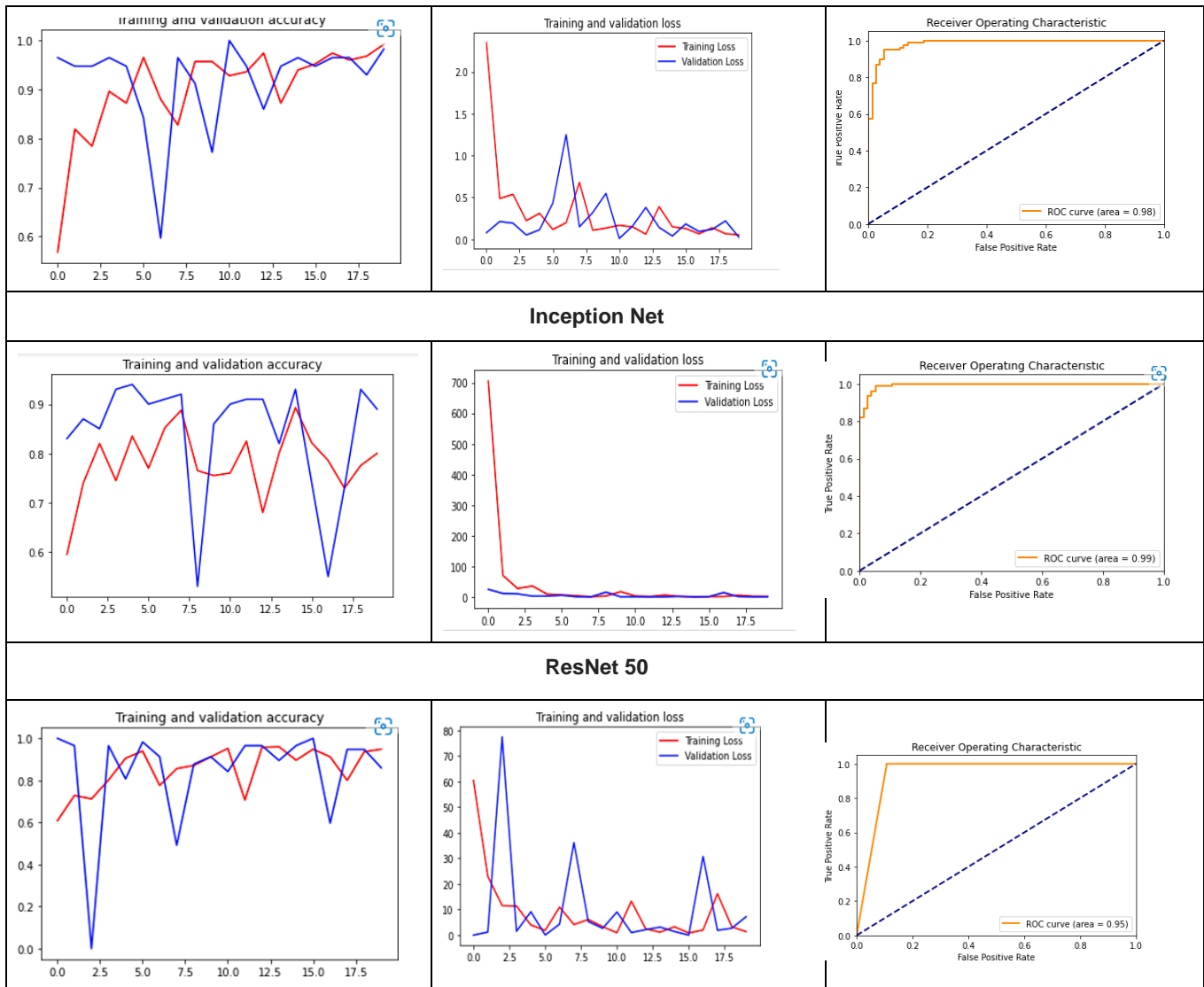


Fig. 8. Performance analysis of considered CNN Models

(First column: training and validation accuracy, Second column: training and validation loss, third column: ROC Curve)

The performance analysis of the AlexNet, VGG net, Mobile Net, InceptionNet and ResNet 50 are presented in the figure 8. From the graphical representations it can be summarized that the pre-trained model Resent50 gives better classification accuracy compared to the other considered models.

From the above analysis, Alex net with a learning rate of 0.001 having 20 epochs gives the highest accuracy of 65% and a minimum loss of 1.1%. It has the lesser efficiency when compared to the other models. MobileNet with a learning rate of 0.01 having 20 epochs gives the highest accuracy of 99% and a minimum loss of 2%. Since the area under the curve is 0.98 and it predominantly lies in the top-left region of the plot and it is inferred that the Mobile Net Classifier has relatively better feature detection abilities compared to the other pre-trained models. VGG Net with a learning rate of 0.001 having 30 epochs yields an accuracy of 85% and a minimum loss of 3%, since the area under the curve is 0.75 it can be inferred that the VGG Net Classifier has relatively lesser feature detection abilities compared to the other pre-trained models. Similarly, the Inception net with a learning rate of 0.01 having 20 epochs gives the highest accuracy of 86% and a minimum loss of 4.2%. It's relatively less in accuracy when compared to MOBILE Net. The AUC is 0.99 which is steep and predominantly close to the top-left corner. However, the ResNet with a learning rate of 0.01 having 20 epochs gives the highest accuracy of 98% and a minimum loss of 1% The AUC is 0.95 that is steep and predominantly close to the top-left corner. Therefore, it is observed that

the ResNet50 have better efficiency towards feature detection abilities with higher accuracy rates and remaining parameters compared to the other pre- trained models.

Table 3. Performance comparison with other pre-trained models

Class Labels N= 198	Class Predicted by the CNN models.									
	Alex net		VGG Net		Mobile Net		Inception Net		ResNet 50	
	TP	TN	TP	TN	TP	TN	TP	TN	TP	TN
PP	112	21	134	4	132	7	139	4	142	3
PN	34	39	12	48	6	45	7	49	4	49
Sensitivity	0.7671		0.9178		0.9565		0.9521		0.9726	
Specificity	0.65		0.9231		0.8654		0.9423		0.9423	
Precision	0.8421		0.971		0.9496		0.9789		0.9793	
Accuracy	0.733		0.9192		0.9316		0.9495		0.9646	
F1 score	0.8029		0.9437		0.9531		0.9653		0.9759	

*PP- Predicted Positive, PN – Predicted Negative, TP- True Positive, TN – True Negative

From the above table, we can infer that ResNet50 has given us the highest accuracy, 96.4%, relative to the other models. We can also observe from the confusion matrices that ResNet50 has performed large values of true positive (142) and true negative (49). AlexNet has the least accuracy, 73.3%, and low values of true positives and true negatives.

4. Conclusion

In this work, the performances of various CNN models in the detection and diagnosis of DFU using thermal imaging modality is studied. The dataset, considered for this work includes images from the 44 control group and 122 diabetic group. The images from the dataset are preprocessed and augmented then fed to the pre trained CNN models. Performance and evaluation metrics were analyzed to determine the best model for DFU detection and diagnosis. Different hyperparameters such as learning rates, epochs and optimizers were used in training the CNN models (AlexNet, VGGNet, Inception Net, ResNet50 and MobileNet). From the analysis, it is inferred that the best model for the aforementioned purpose is ResNet50. Further, This research can also be expanded to track the disease's development using real-time data.

Acknowledgement

The authors would like to thank the management of Sri Sivasubramaniya Nadar College of Engineering, Kalavakkam, for providing the facilities to carry out this work.

REFERENCES

- [1] Baig MS, et al. An Overview of Diabetic Foot Ulcers and Associated Problems with Special Emphasis on Treatments with Antimicrobials. Life (Basel). 2022 Jul 14;12(7):1054. doi: 10.3390/life12071054.
- [2] Aumiller, et al, Pathogenesis and management of diabetic foot ulcers. JAAPA 28(5):p 28-34, May 2015. | DOI: 10.1097/01.JAA.0000464276.44117.b1

- [3] Wang X, et al. Diabetic foot ulcers: Classification, risk factors and management. *World J Diabetes*. 2022 Dec 15;13(12):1049-1065. doi: 10.4239/wjd.v13.i12.1049
- [4] Yang L, et al. Diabetic foot ulcer: Challenges and future. *World J Diabetes*. 2022 Dec 15;13(12):1014-1034. doi: 10.4239/wjd.v13.i12.1014.
- [5] Said G. Diabetic neuropathy. *Handb Clin Neurol*. 2013;115:579–589.
- [6] Ahmad Abu Alrub, et al "Factors Associated with Health-Related Quality of Life among Jordanian Patients with Diabetic Foot Ulcer", *Journal of Diabetes Research*, vol. 2019, Article ID 4706720, 8 pages, 2019. <https://doi.org/10.1155/2019/4706720>
- [7] Dane K. Wukich et al Assessing Health-Related Quality of Life in Patients With Diabetic Foot Disease: Why Is It Important and How Can We Improve? The 2017 Roger E. Pecoraro Award Lecture. *Diabetes Care* 1 March 2018; 41 (3): 391–397.
- [8] Alosaimi, F.D., et al. Associations of foot ulceration with quality of life and psychosocial determinants among patients with diabetes; a case-control study. *J Foot Ankle Res* 12, 57 (2019). <https://doi.org/10.1186/s13047-019-0367-5>
- [9] Perez Calvo C, Garcia-García B, Marrugo-Padilla V, Montes-Sierra D, Alvarado-Castell H, (2021) Diabetic Foot Tools for the Identification of the Foot at Risk and its Timely Intervention., *Arch de Medi* . Vol: 17 No: 7
- [10] Wang Y, Shao T, Wang J, Huang X, Deng X, Cao Y, Zhou M, Zhao C. An update on potential biomarkers for diagnosing diabetic foot ulcer at early stage. *Biomed Pharmacother*. 2021 Jan;133:110991. doi: 10.1016/j.biopha.2020.110991.
- [11] Sun H, Saeedi P, Karuranga S, Pinkepank M, Ogurtsova K, Duncan BB, Stein C, Basit A, Chan JCN, Mbanya JC, Pavkov ME, Ramachandaran A, Wild SH, James S, Herman WH, Zhang P, Bommer C, Kuo S, Boyko EJ, Magliano DJ. IDF Diabetes Atlas: Global, regional and country-level diabetes prevalence estimates for 2021 and projections for 2045. *Diabetes Res Clin Pract*. 2022 Jan;183:109119. doi: 10.1016/j.diabres.2021.109119.
- [12] Boulton AJ, et al; American Diabetes Association; American Association of Clinical Endocrinologists. Comprehensive foot examination and risk assessment: a report of the task force of the foot care interest group of the American Diabetes Association, with endorsement by the American Association of Clinical Endocrinologists. *Diabetes Care*. 2008 Aug;31(8):1679-85. doi: 10.2337/dc08-9021.
- [13] Vitalii I. et al CURRENT ASPECTS OF URGENT SURGICAL ASSISTANCE IN PATIENTS WITH DIABETIC FOOT SYNDROME, *Emergency Medical Service*, 10.36740/EmeMS202301103, 10, 1, (22-27), (2023).
- [14] Siying Liu et al, Analysis for warning factors of type 2 diabetes mellitus complications with Markov blanket based on a Bayesian network model, *Computer Methods and Programs in Biomedicine* Volume 188, May 2020, 105302.
- [15] Wang A, Lv G, Cheng X, Ma X, Wang W, Gui J, Hu J, Lu M, Chu G, Chen J, Zhang H, Jiang Y, Chen Y, Yang W, Jiang L, Geng H, Zheng R, Li Y, Feng W, Johnson B, Wang W, Zhu D, Hu Y. Guidelines on multidisciplinary approaches for the prevention and management of diabetic foot disease (2020 edition). *Burns Trauma*. 2020 Jul 6;8:tkaa017. doi: 10.1093/burnst/tkaa017.
- [16] Rajmanova, P., Nudzikova, P., & Vala, D. (2015). Application and technology of thermal imagine camera in medicine. *IFAC-PapersOnLine*, 48(4), 492-497.
- [17] Fraiwan L, AlKhodari M, Ninan J, Mustafa B, Saleh A, Ghazal M. Diabetic foot ulcer mobile detection system using smart phone thermal camera: a feasibility study. *Biomed Eng Online*. 2017 Oct 3;16(1):117. Doi:
- [18] Infrared Technology". thermalscope.com. Archived from the original on 8 November 2014.
- [19] Seuser A, Kurnik K, Mahlein AK. Infrared Thermography as a Non-Invasive Tool to Explore Differences in the Musculoskeletal System of Children with Hemophilia Compared to an Age-Matched Healthy Group. *Sensors (Basel)*. 2018 Feb 8;18(2):518. doi: 10.3390/s18020518.

- [20] Yunze He, et al, Infrared machine vision and infrared thermography with deep learning: A review, *Infrared Physics & Technology* Volume 116, August 2021, 103754.
- [21] FLIR x8500sc Thermal imaging camera specifications.2019-07-10.
- [22] D. A. Hernandez-Contreras, H. Peregrina-Barreto, J. d. J. Rangel-Magdaleno and F. J. Renero-Carrillo, "Plantar Thermogram Database for the Study of Diabetic Foot Complications," in *IEEE Access*, vol. 7, pp. 161296-161307, 2019, doi: 10.1109/ACCESS.2019.2951356.
- [23] Cai, Lei, et al. "A review of the application of deep learning in medical image classification and segmentation." *Annals of translational medicine* vol. 8,11 (2020): 713. doi:10.21037/atm.2020.02.44
- [24] Keshana, Hasitha. (2021). A Review on Applications of Convolutional Neural Network (CNN) in Oncology.
- [25] A. Victor Ikechukwu, ResNet-50 vs VGG-19 vs training from scratch: A comparative analysis of the segmentation and classification of Pneumonia from chest X-ray images, *Global Transitions Proceedings* Volume 2, Issue 2, November 2021, Pages 375-381
- [26] Pandit, Tejas & Kapoor, Akshay & Shah, Rishi & Bhuvra, Rushi. (2020) Understanding Inception Network Architecture For Image Classification. 10.13140/Rg.2.2.16212.35204.
- [27] C. Szegedy *et al.*, "Going deeper with convolutions," *2015 IEEE Conference on Computer Vision and Pattern Recognition (CVPR)*, Boston, MA, USA, 2015, pp. 1-9, doi: 10.1109/CVPR.2015.7298594.
- [28] Ayesha Younis, Li Shixin, Shelembi Jn, and Zhang Hai. 2020. Real-Time Object Detection Using Pre-Trained Deep Learning Models MobileNet-SSD. In *Proceedings of 2020 6th International Conference on Computing and Data Engineering (ICCD E'20)*. Association for Computing Machinery, New York, NY, USA, 44–48
- [29] Howard, Andrew & Zhu, Menglong & Chen, Bo & Kalenichenko, Dmitry & Wang, Weijun & Weyand, Tobias & Andreetto, Marco & Adam, Hartwig. (2017). *MobileNets: Efficient Convolutional Neural Networks for Mobile Vision Applications*.